Supplementary Material (ESI) for Dalton Transactions
This journal is © The Royal Society of Chemistry

Two new POM-based compounds constructed by rigid thiabendazole and flexible bis(pyrazole) ligands: structures and properties for Hg^{2+} recognition

Aixiang Tian,* Yali Ning, Yang Yang, Xue Hou, Jun Ying, Guocheng Liu, Juwen Zhang, Xiuli Wang*

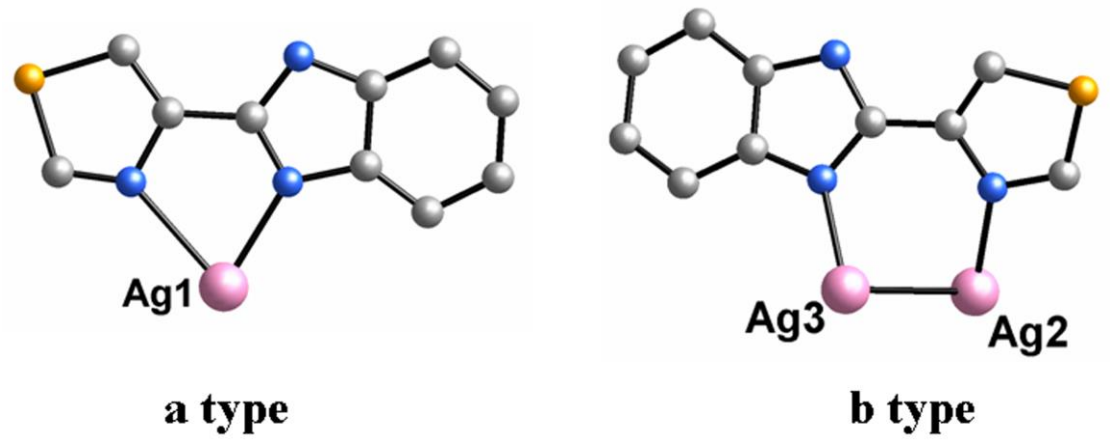

Fig. S1. Two types of coordination modes of tbz ligand in compound **1**.

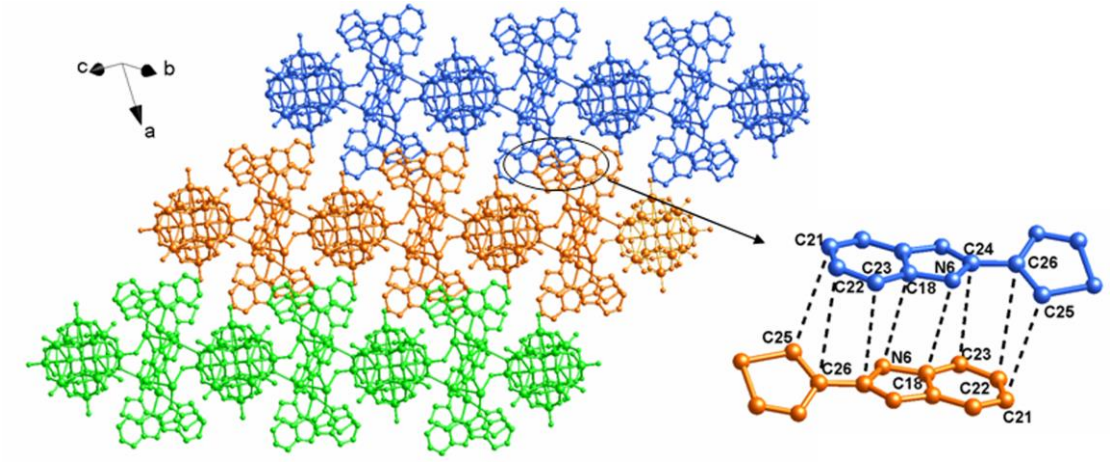

Fig. S2. A 2D supramolecular layer in **1** constructed by abundant π…π stacking interactions between adjacent 1D chains.

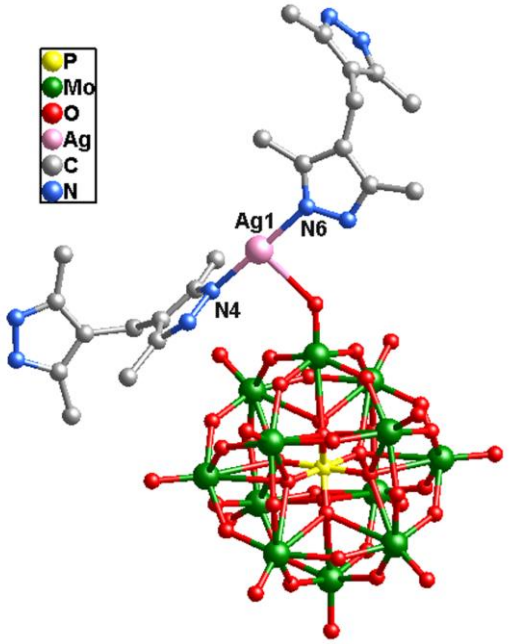

Fig. S3. Ball/stick view of the asymmetric unit of **2**. The hydrogen atoms and crystal water molecules are omitted for clarity.

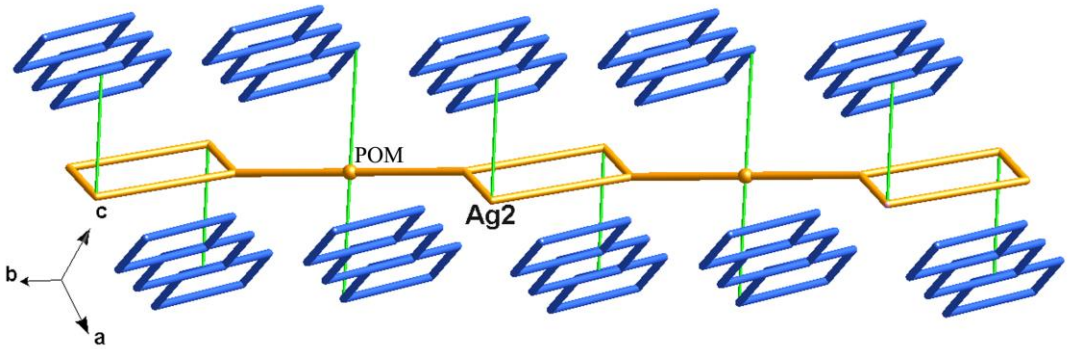

Fig. S4. The chain (orange) is vertical with its adjacent linking chains (blue).

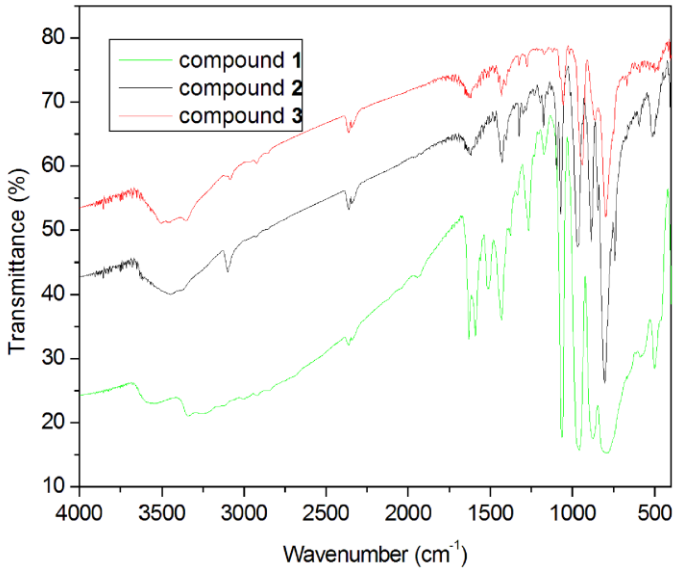

Fig. S5. The IR spectra of compounds **1–3**.

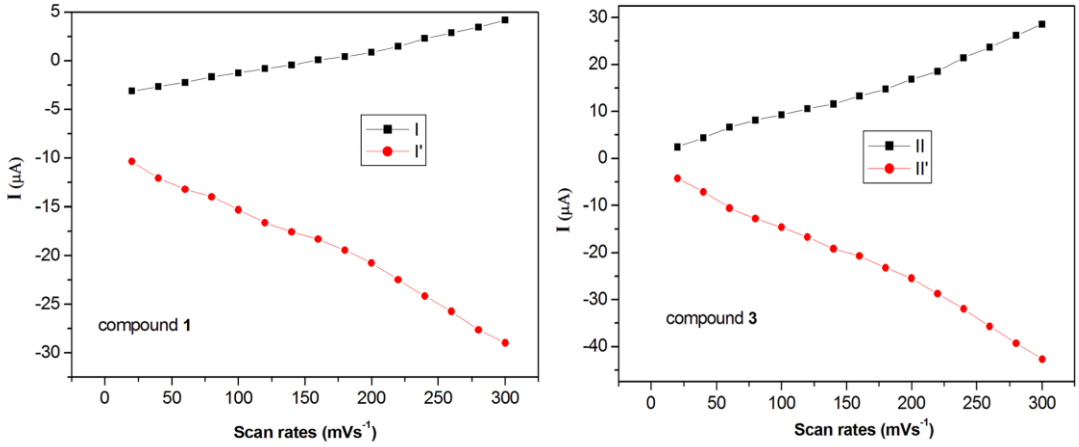

Fig. S6. The dependence of anodic peak (I for **1**–CPE, II for **3**–CPE) and cathodic peak (I' for **1**–CPE, II' for **3**–CPE) currents on scan rates.

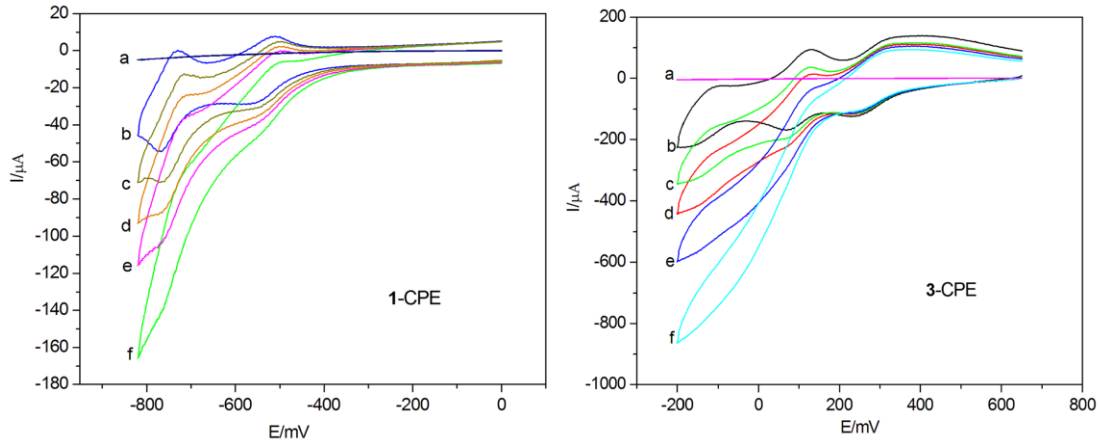

Fig. S7. Cyclic voltammograms of the **1**– and **3**–CPEs in 0.1M H_2SO_4 + 0.5M Na_2SO_4 aqueous solution containing 0(b); 2(c); 4(d); 6(e) and 8(f) mM H_2O_2 and a bare CPE (a) in a 4.0 mM H_2O_2 + 0.1M H_2SO_4 + 0.5M Na_2SO_4 solution. Scan rate: 200 $mV \cdot s^{-1}$.

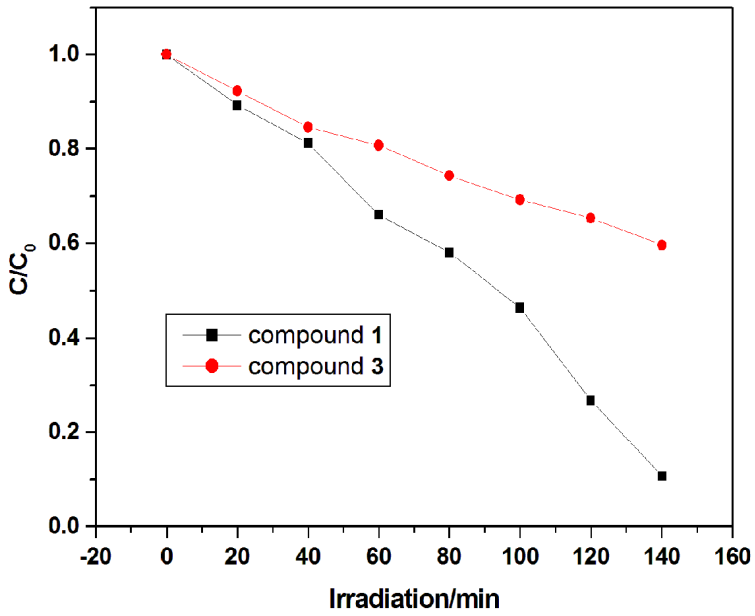

Fig. S8. Photocatalytic decomposition rate of the MB solution under UV irradiation with the use of the title compounds **1** and **3**.

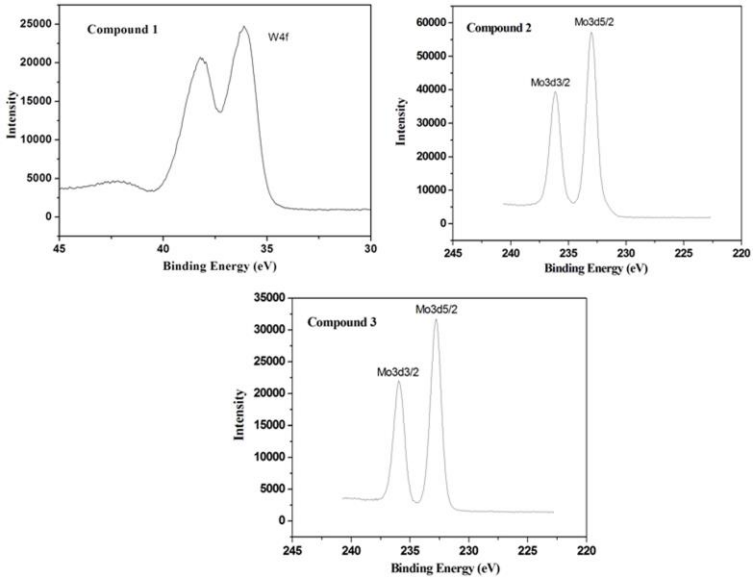

Fig. S9. The XPS spectra of compounds **1**–**3** and the results exhibit that the oxidation states of Mo and W atoms in compounds **1**–**3** are in +VI oxidation state.

Table S1. Selected Bond Lengths (Å) and Bond Angles (°) for Compounds **1**–**3**.

		Compound **1**	
Ag1-N1	2.105(9)	Ag1-N5	2.160(9)
Ag1-N3	2.454(11)	Ag1-Ag2	3.1452(14)
Ag2-C7	2.149(9)	Ag2-N8	2.150(9)
Ag2-Ag3	2.9334(14)	Ag2-O9	2.773(3)
Ag3-N2	2.153(9)	Ag3-N7	2.152(9)
Ag3-O7	2.763(11)	C26-S2	1.710(12)
C27-S2	1.678(12)	S1-C9	1.699(16)
S1-C8	1.718(17)	N1-Ag1-N5	161.4(4)
N1-Ag1-N3	125.1(4)	N5-Ag1-N3	73.0(4)
N1-Ag1-Ag2	63.3(3)	N5-Ag1-Ag2	100.2(3)
N3-Ag1-Ag2	141.6(3)	C7-Ag2-N8	171.9(4)
C7-Ag2-Ag3	100.4(3)	N8-Ag2-Ag3	78.5(2)
C7-Ag2-Ag1	65.7(3)	N8-Ag2-Ag1	106.2(2)
Ag3-Ag2-Ag1	91.12(4)	N2-Ag3-N7	149.0(3)
N2-Ag3-Ag2	84.6(3)	N7-Ag3-Ag2	85.6(2)
C9-S1-C8	89.3(7)	C27-S2-C26	89.6(6)
		Compound **2**	
Ag1-N5	2.122(6)	Ag1-N1	2.134(7)
N5-Ag1-N1	176.9(3)		
		Compound **3**	
Ag1-N5	2.134(5)	Ag1-N3	2.173(6)
Ag1-Ag2	3.2165(10)	Ag1-O8	2.663(6)
Ag2-N6	2.115(6)	Ag2-N2	2.120(6)
Ag2-O20	2.744(6)	C10-S1	1.671(13)
C9-S1	1.698(9)	N5-Ag1-N3	178.6(3)

N5-Ag1-Ag2	100.19(16)	N3-Ag1-Ag2	78.4(2)
N6-Ag2-N2	167.6(3)	N6-Ag2-Ag1	120.65(19)
N2-Ag2-Ag1	68.84(19)	C10-S1-C9	90.4(5)

Table S2. The Mo and W oxidation states in compounds **1**–**3** through BVS.

1		**2**				**3**	
W1	6.431	Mo1	6.202	Mo7	6.355	Mo1	6.311
W2	6.396	Mo2	6.235	Mo8	6.314	Mo2	6.167
W3	6.537	Mo3	6.438	Mo9	6.453	Mo3	6.263
W4	6.671	Mo4	6.491	Mo10	6.429	Mo4	6.176
W5	6.453	Mo5	6.277	Mo11	6.467	Mo5	6.066
W6	6.555	Mo6	6.677	Mo12	6.779	Mo6	6.531